VIP Photonic Crystals

DOI: 10.1002/anie.200804391

Electroactive Inverse Opal: A Single Material for All Colors**

Daniel P. Puzzo, Andre C. Arsenault, Ian Manners, and Geoffrey A. Ozin**

Photonic crystals (PCs)[1,2] made by bottom-up self-assembly and top-down nanofabrication approaches have been receiving increasing attention across the science and engineering disciplines in academia and industry. They have been envisioned for a range of applications including optical transistors and waveguides,[3,4] light-emitting diodes and lasers,[5,6] chemical and biochemical sensors,[7,8] and data storage media.[9] A challenge in the field has been the realization of PCs for full-color reflective displays which could be used for electronic books, billboards, shelf-edge labels, and state-of-health fuel gauges for batteries. To reduce this objective to practice requires an active PC whose refractive index contrast and/or lattice dimension can be continuously, reversibly, and rapidly altered by an electrical, optical, or magnetic stimulus, and that can be prepared with high structural and optical quality, and on a large scale at low cost.

There have been a few early attempts at achieving these objectives. One involves an electrically tuned liquid crystal imbibed within the void spaces of an inverse silica opal; however, this device is limited as it is able to switch between just two colors corresponding to random and aligned director fields.[10] Another involves magnetic tuning of the spacing between an ordered dispersion of superparamagnetic iron oxide microspheres; however, while full-color magnetic tuning was demonstrated, it is difficult to envision how this dispersion can be made into a practical display.[11] The first demonstration of full-color tuning of a PC was based on an electroactive polymer-gel/silica opal composite, the reflected color of which can be electrically tuned through reversible expansion and contraction of its photonic lattice.[12] The problem with this system relates to the difficulty of electrolyte permeating through a contiguous space-filling opal lattice made of close-packed silica spheres embedded within a polymer-gel matrix. This construct impedes electron and ion charge transport, slows switching times, and increases the drive voltage needed to power the device, all together negating the overall performance of the device.

Herein we describe the first example of a high-performance electroactive inverse polymer-gel opal in which electrolyte freely infuses the nanoporous lattice. The positive outcome is the reduction in electron and ion diffusion lengths, the increase in switching speed, and the decrease in the driving voltage, with unprecedented tuning of the wavelength and brightness of Bragg diffracted light continuously from the invisible ultraviolet through the visible to the invisible near infrared.

The structures of the polymers chosen for the inverse polymer-gel opal in this study are shown in Figure 1b. They comprise the polyferrocenylsilane (PFS) derivatives polyferrocenylmethylvinylsilane (PFMVS) and polyferrocenyldivinylsilane (PFDVS); narrow polydispersity index (PDI < 1.1) and molecular weight control are achieved through anionic ring-opening polymerization from the appropriate silaferrocenophanes. Under anionic polymerization conditions, ring-opening of the silaferrocenophane is favored over addition to the carbon–carbon double bonds present in each monomer unit leaving the latter intact.[13] It is necessary that pendant carbon–carbon double bonds be present along the polymer backbone to enable cross-linking through the well-known thiol–ene process.

The methodology used to prepare the inverse polymer-gel opals is outlined in Figure 1a. First, an opal film made of monodisperse silica spheres was deposited on glass by evaporation-induced self-assembly.[14] A scanning electron microscopy (SEM) image effectively confirms the *fcc* close packing of the silica spheres (Figure 1d). The void volume of the prepared silica opal was then infiltrated with a solution containing either one of the two polymers bearing terminal C=C bonds, a small amount of a di- or trifunctional thiol, and a photoinitiator. The composite was subsequently exposed to ultraviolet light in order to cross-link the polymer chains by a thiol–ene reaction to afford a polymer-gel/silica opal composite. After cross-linking and removal of the polymer overlayer, the silica spheres of the polymer/silica composites were removed upon treatment with 1–2% hydrofluoric acid. Because the composites are mounted on glass, HF etching yields free-standing inverse polymer-gel opals, which were subsequently collected onto indium tin oxide (ITO)-coated glass for subsequent electrical analysis and actuation. Figure 1e includes an SEM image of the resulting inverse polymer-gel opal which reveals a periodic structure consisting of a network of ordered macropores connected to one another by ordered mesopores corresponding to the silica microspheres and where they touched, respectively.

[*] I. Manners
School of Chemistrty, University of Bristol
Cantock's Close, Bristol, BS8 1TS (UK)
E-mail: ian.manners@bris.ac.uk

D. P. Puzzo, G. A. Ozin
Department of Chemistry, University of Toronto
80 St. George Street, Toronto, M5S 3H6 (Canada)
Fax: (+1) 416-971-2011
E-mail: gozin@chem.utoronto.ca

A. C. Arsenault
Opalux Inc., Department of Chemistry, University of Toronto
80 St. George Street, Toronto, M5S 3H6 (Canada)

[**] G.A.O. holds a Government of Canada Research Chair in Materials Chemistry. He is deeply grateful to the Natural Sciences and Engineering Research Council of Canada NSERC for generous and sustained funding of his research. I.M. thanks the EU for a Marie Curie Chair. D.P.P. would like to thank W. Wang for the schematics provided and the University of Toronto for financial support.

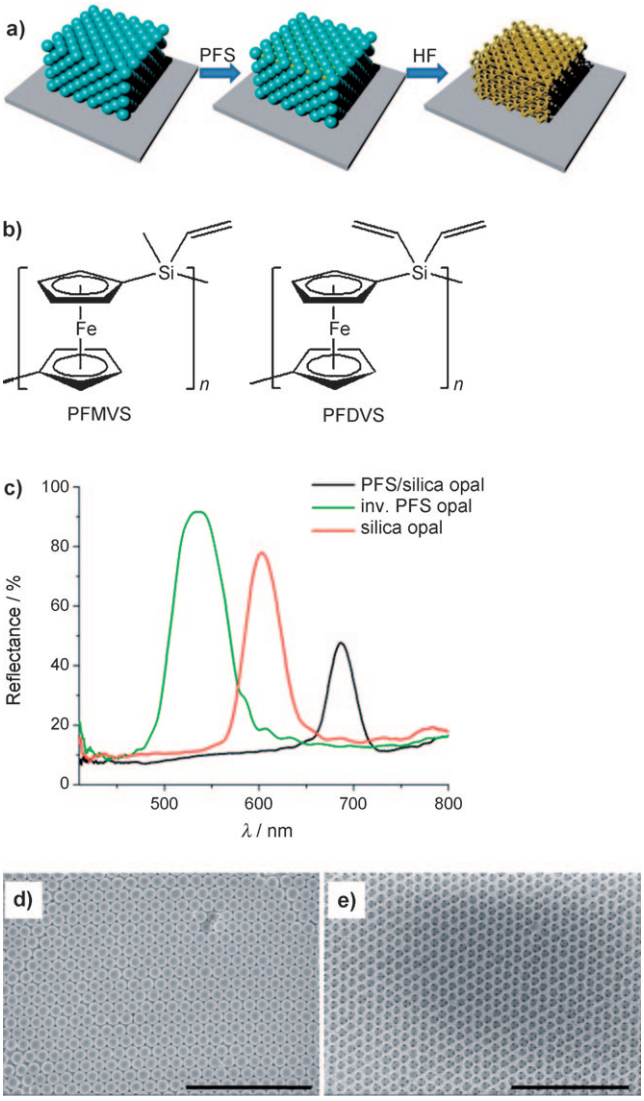

Figure 1. a) Representation of the preparation of PFS-based inverse opals. b) Molecular structure of the electroactive polymers employed in active opals. c) Evolution of the Bragg peak throughout fabrication of inverse opal; the green curve corresponds to the inverse polymer-gel opal, the red curve the silica opal, and the black curve the polymer-gel/silica opal composite. d) SEM image of a silica opal prepared with silica spheres 270 nm in diameter. e) SEM image of an inverse polymer-gel opal templated by silica spheres 270 nm in diameter. Scale bars of (d) and (e) represent 3 μm.

Reflectance spectra recorded at various points throughout the inverse opal fabrication process are shown in Figure 1c. The red curve centered at 603 nm corresponds to the reflectance spectrum of the bare opal prepared from silica spheres with a diameter of 270 nm. Following infiltration of the opal with the PFMVS or PFDVS polymer gel, the reflectance of the resulting composite (black curve with a stopband maximum at 686 nm) is red-shifted by 84 nm and the stopband intensity decreases by 30% relative to the spectrum of the bare silica opal. Finally, the desired polymer inverse opal exhibits a Bragg reflectance peak centered at 538 nm which is blue-shifted by 65 nm and 150 nm relative to the analogous peaks of the bare silica opal and polymer-gel/silica opal composite, respectively. These observed changes in the reflectance spectra from one material to another in the series are attributed entirely to differences in refractive index contrast between the opaline lattice and the material (or lack thereof) in the interstitial void volume. The reflectance spectra agree well with the theoretical prediction of the Bragg–Snell equation [Eq. (1)]. Here, λ is the central wavelength of reflected or transmitted light, n_{eff} is the volume-weighted average of the refractive index of the constituent opal spheres and what occupies the interstitial voids [$n_{eff} = (0.74\,n_{sphere} + 0.26\,n_{void})$], D is the distance between 111 lattice planes given by $D = \sqrt{(2/3)}d$ where d is the diameter of a sphere, and θ is the Bragg angle of incidence of the light on the opal. It is assumed that the spheres and air occupy 74% and 26%, respectively, of the total film volume.[15]

$$\lambda = 2\,D(n_{eff}^2 - \cos^2\theta)^{1/2} \quad (1)$$

Figure 2 includes cyclic voltammograms of samples of equal area (1 cm × 1 cm) and thickness (5.2 μm) of a polymer-gel opal film and a polymer-gel/silica opal film on ITO-coated glass. The voltammograms were acquired in a three-electrode configuration and overlayed for comparative purposes. Both materials display electrochemical features characteristic of main-chain ferrocene-based polymers, exhibiting two broad and overlapping redox waves.[16] The obvious difference, however, is that the peak current measured for the inverse polymer-gel opal (dark curve) is larger than that of the polymer-gel opal composite (lighter curve). This indicates that a greater area is sampled over the timescale of the CV measurement in the inverse polymer-gel opal, which most likely can be attributed to its significantly enhanced electron and ion transport compared to that of the polymer-gel opal

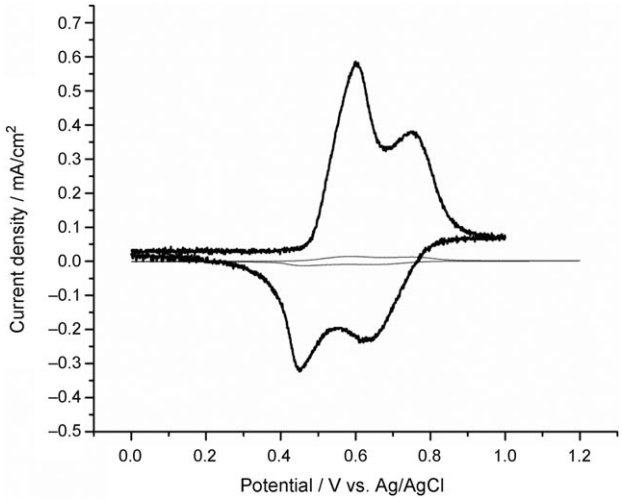

Figure 2. Cyclic voltammograms of films of equal area (1 cm × 1 cm) and thickness (5.2 μm) on ITO-coated glass of a inverse polymer-gel opal and a polymer-gel/silica opal composite; the cyclic voltammograms were acquired in a three-electrode configuration and overlayed for comparative purposes; scan rate: 10 $mV^{-1}s$. The darker curve corresponds to the inverse opal and the lighter curve corresponds to the polymer opal composite.

composite. Such transport properties are desirable for a range of active opal applications as they are expected to improve overall device performance, as the remainder of this report will attest.

Electrical tuning was achieved by fabricating a button cell consisting of inverse polymer-gel opal supported on ITO glass which served as the working electrode; this was separated from an ITO-glass or FTO-glass counterelectrode by a hot-melt ionomer spacer (Dupont). The cell was filled with a liquid electrolyte and sealed. Potentials were applied to the cell by connecting the top face of each electrode to the leads of a potentiostat or another suitable power supply (Figure 3a).

The inverse polymer-gel opal exhibited voltage-dependent diffraction characteristics similar to those of the polymer-gel opal composite. For example, when an oxidative potential (a potential more positive than the redox potential of the polymer) is applied to the electrode bearing the polymer-gel opal composite, electrons are extracted from the iron atoms in the polymer backbone while anions from the electrolyte diffuse into the polymer in order to maintain charge neutrality. The influx of both ions and solvent into the polymer causes it to swell and push apart the layers of spheres, and the reflected optical diffraction peak is red-shifted. Applying a reducing potential drives the reverse process, with electrons being injected back into the polymer and the anions being expelled out into the electrolyte. This same mechanism is operative in the inverse polymer-gel opal, and hence its optical behavior is similar to that of the polymer-gel opal composite. The plot in Figure 3b illustrates the ability of the inverse polymer-gel opal film to display voltage-dependent continuous shifts in reflected light as the Bragg peak is swept throughout the entire visible spectrum with voltages in the range 1.2 V–2.8 V applied in 0.1 V increments.

While the inverse and normal polymer-gel opals both display voltage-tuneable structural color, the former is notably superior in all aspects of device performance. First, the range over which the stopband of the inverse polymer-gel opal with a cross-linker concentration of 5 mol% and under an applied bias of 2.8 V was observed to be approximately 300 nm (see Figure 4). In contrast, a tuning range of only 210 nm at a significantly lower cross-linker concentration of 0.5 mol% and a larger bias of 3.2 V was observed with the polymer-gel opal composite. Second, a significantly larger color-tuning range was accessible at significantly lower potentials for the inverse polymer-gel opal than for the polymer-gel opal composite. For example, at a cross-linker concentration of 10 mol% and under an applied voltage of 2.4 V, the former displayed a peak-to-peak shift of 240 nm, whereas the latter, at a cross-linker concentration of 0.5 mol% and under a 2.4 V bias, showed a shift of 100 nm. Third, these results are scientifically important and technologically significant not only because a 300 nm tuning range implicates the fabrication of a single PC device capable of spanning the entire visible spectrum, namely a single material for all colors (Figure 3a and b), but also because the stability (mechanical, thermal, electrochemical) of the polymer gel in such devices has been observed to improve with increasing cross-linker content. As samples with low cross-linker densities suffer from instability, use of lightly cross-linked samples is impractical from a commercial perspective. It is much more desirable to fabricate a device consisting of a suitably cross-linked polymer gel in the 5–10 mol% range to ensure stability which is simultaneously capable of swelling to the extent necessary for full-color tuning.

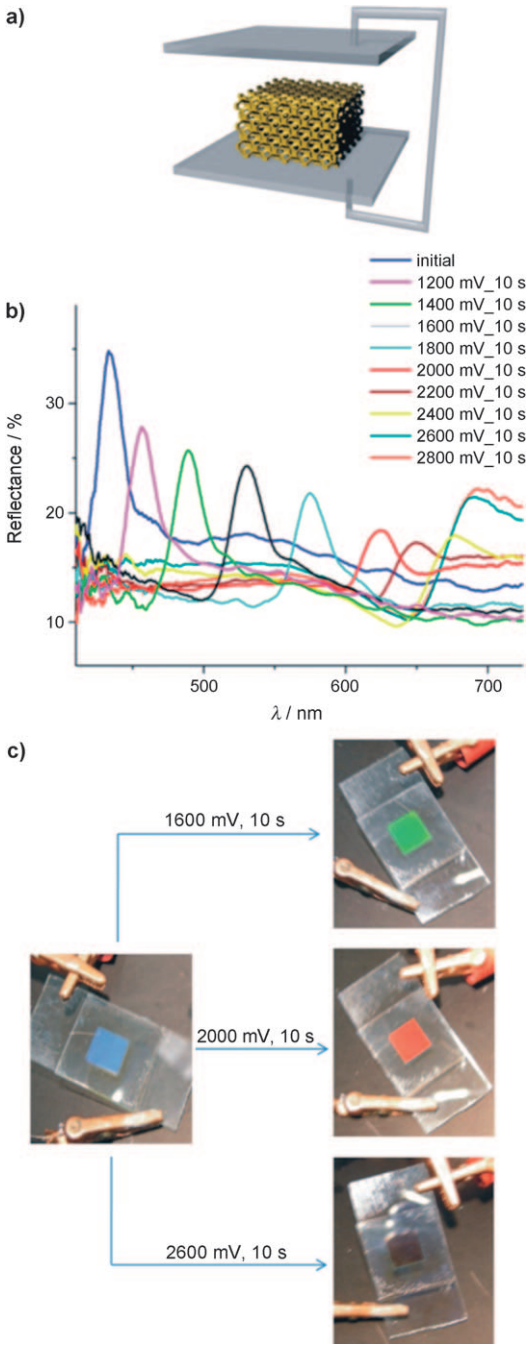

Figure 3. a) Representation of the electrochemical cell fabricated for the electrical actuation of the active inverse opal. Proof of full-color tuning by recorded spectra (b) and photographs (c) of the cell. The cross-linker concentration in this sample was 10 mol%.

The impressive performance of the inverse polymer-gel opal is attributed primarily to its highly porous structure which increases the specific surface area of the film in contact

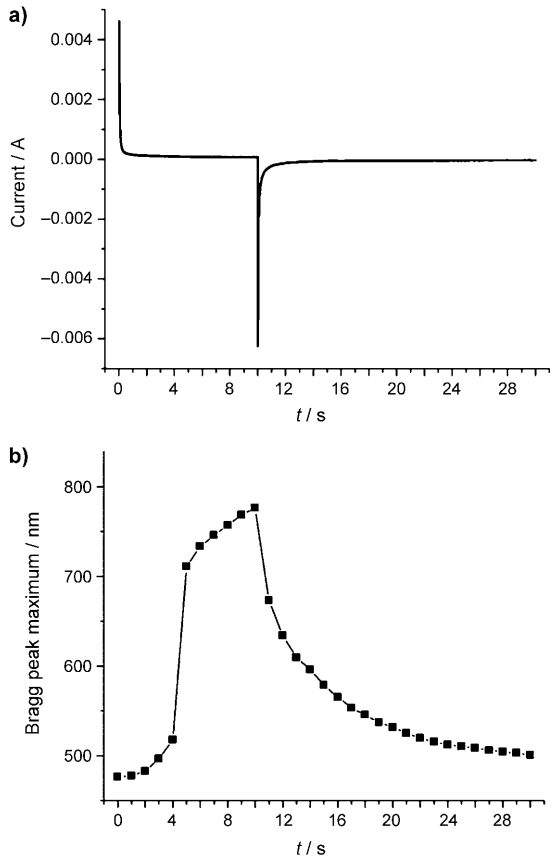

Figure 4. a) The chronoamperometric response of the two-electrode inverse polymer-gel opal device upon application of two potential steps, the first at 2.6 V for 10 s and the second at −2.8 V for 20 s. b) Evolution of the Bragg peak maximum with time over the same time intervals as in (a). The cross-linker concentration for this sample was 5 mol%.

with electrolyte. In sharp contrast, in the polymer-gel opal composite the electrolyte is in contact only with the top surface of the film prior to electrical actuation. Therefore, in order for the polymer gel to swell completely and homogeneously, on application of a positive potential to the film, ions are forced to diffuse all the way through an effectively nonporous matrix of polymer and silica opal to find the electrode surface, a distance which can fall anywhere in the range of 5–10 μm. However, for an inverse polymer-gel opal the ordered interconnected macropores and mesopores extend throughout the entire electroactive material, and thereby the diffusion lengths of electrons and ions into and out of the polymer gel necessary for maximal swelling of the inverse opal lattice are decreased. The overall effect of such enhanced diffusion capacity is a decrease in the cell resistance as is evident by the lower potentials necessary to drive the device (as described above).

The kinetics of the stopband tuning of a 5 mol% cross-linked inverse polymer-gel opal were investigated. The plot in Figure 4a shows the chronoamperometric response of the two-electrode device, which essentially includes the monitoring of the current running through the device upon application of two potential steps. In this experiment, the current was first measured following application of a potential step of 2.6 V over a 10 s interval (corresponding to the forward scan) followed by an instantaneous polarity switch with an application of −2.8 V potential step for 20 s (corresponding to the reverse scan). The rapid decay of the current from an initial value (observed with both the forward and reverse biasing) and acquisition of diffusion control almost immediately following biasing is testament to the good electronic conduction and ionic mobility present in the polymer gel. In addition to the current, the Bragg peak shift was also monitored over the same time range of the applied voltage pulses (Figure 4b). Initially, upon application of the 2.6 V forward bias, swelling of the polymer gel with concomitant red-shifting of the stopband is relatively minute, with a shift of only 41 nm occurring after 4 s of biasing. At the 4 s instant, however, a dramatic red-shift of 194 nm is observed over a 1 s interval followed by a tapering of the stopband response with the remainder of the forward biasing. The large stopband shift at 4 s is believed to occur as a result of a significant increase in the hole conductivity of the polymer gel originating from a *p*-doping effect. At the 10 s mark, the polarity is switched in order to reverse the swelling process and monitor the kinetics of the contraction of the polymer gel to its original state. The most significant blue-shift is observed initially as soon as the polarity is reversed. As the negative bias is continually applied, blue-shifting persists relatively slowly with a lesser shift occurring with each passing second. The more sluggish behavior of the reverse scan is attributed primarily to the *p*-type character of the polymer (which is believed to be a poor conductor of electrons) as well as a "de-doping effect".[17] For other voltages, similar stopband shift versus time profiles were obtained, the only difference being that larger shifts were observed with larger applied voltages for the same time intervals in accordance with the data displayed in Figure 3b.

Herein we have described the first example of an electroactive inverse opal that offers full color at very low drive voltages with unprecedented wavelength shifts traversing the ultraviolet, visible, and near infrared spectral ranges. Technological hurdles to be overcome include reflectivity enhancement, boosting the speed of the reverse scan, and increasing the cycle lifetime. Adding nanoparticles to the polymer gel can enhance color contrast and provide control over the viewing angle, while tailoring the device components can reduce cell resistance and enable full-color tuning with applied voltages below 2 V.

Experimental Section

Cyclic voltammograms were obtained with a BAS epsilon potentiostat from a three-electrode configuration with the inverse opal on ITO, a platinum wire, and a silver/silver chloride electrode serving as the working, the counter, and the reference electrodes, respectively. The solvent/electrolyte for cyclic voltammetry was acetonitrile/tetrabutylammonium hexafluorophosphate (0.3 M). Optical spectra were acquired with an Ocean Optics SD2000 fiber optic spectrophotometer coupled to an optical microscope.

Synthesis of polyferrocenylmethylvinylsilane (PFMVS) and polyferrocenyldivinylsilane (PFDVS): Polymerizations were performed under standard anionic polymerization[13] conditions, and more complete details of the syntheses of these polymers will be provided

in a future publication. Briefly, in a glove box, 300 mg of the appropriate silaferrocenophane (either divinylsilaferrocenophane or methylvinylsilaferrocenophane) was dissolved in 3 mL of anhydrous THF. This solution was treated with 7 μL of 1.6 M *n*-butyllithium. The reaction was allowed to proceed for 45 min before it was quenched with degassed methanol. The desired polymer was then precipitated from methanol (80% yield, PDI = 1.09, M_n = 24 KDa).

Preparation of an inverse PFS polymer-gel: Firstly, an opal film made of monodisperse silica spheres was deposited on glass by evaporation-induced self-assembly.[14] To acquire an initial reflectance of blue, films were grown from 180 nm silica spheres prepared at a concentration of 1 vol%. The void volume of the prepared silica opal was then infiltrated with a concentrated solution (1 mg of polymer in 4 μL of solution) containing either one of the two polymers bearing terminal C=C bonds, 5—10 mol% 1,4-butanedithiol, and 1 mol% Igracure in toluene. The composite was subsequently exposed to ultraviolet light for 10 h in order to cross-link the polymer chains to afford a polymer-gel/silica opal composite. After cross-linking, the silica spheres of the polymer/silica composites were removed by immersing the prepared films in 1–2% hydrofluoric acid for 10 min. The resulting free-standing inverse polymer-gel opals were then subsequently collected onto ITO-coated glass for electrical analysis and actuation.

Cell design: The cell employed was a simple two-electrode electrochemical cell[18,19] with the inverse opal on ITO serving as the working electrode and a bare ITO electrode serving as the counter electrode. The two electrodes were fused together with a 4 mil. Surlyn hot-melt spacer (Dupont) which was cut in the form of a frame for the inverse opal material such that there was a single gap to separate the two electrodes of the cell. A droplet of electrolyte (glutaronitrile/lithium hexafluorophosphate 0.3 M) was then placed against this gap (where it beaded as a result of surface tension) and then the cell was placed inside a desiccator. The desiccator was then evacuated (which also effectively evacuated the cell) and then filled with N_2, the pressure of which pushed the liquid into the cell.

Received: September 5, 2008
Revised: October 8, 2008
Published online: December 3, 2008

Keywords: conducting materials · inverse opals · liquid crystals · photonic crystals

[1] E. Yablonovitch, *Phys. Rev. Lett.* **1987**, *58*, 2059 – 2062.
[2] S. John, *Phys. Rev. Lett.* **1987**, *58*, 2486 – 2489.
[3] D. Dragoman, M. Dragoman, *Prog. Quantum Electron.* **1999**, *23*, 131.
[4] E. Centeno, D. Felbacq, *Opt. Commun.* **1999**, *160*, 57 – 60.
[5] J. M. Weissman, H. B. Sunkara, A. S. Tse, S. A. Asher, *Science* **1996**, *274*, 959 – 960.
[6] E. A. Kamenetzky, L. G. Magliocco, H. P. Panzer, *Science* **1994**, *263*, 207 – 210.
[7] J. H. Holtz, S. A. Asher, *Nature* **1997**, *389*, 829 – 832.
[8] S. A. Asher, V. L. Alexeev, A. V. Goponenko, A. C. Sharma, I. K. Lednev, C. S. Wilcox, D. N. Finegold, *J. Am. Chem. Soc.* **2003**, *125*, 3322 – 3329.
[9] O. D. Velev, E. W. Kaler, *Langmuir* **1999**, *15*, 3693 – 3698.
[10] S. Kubo, Z.-Z. Gu, K. Takahashi, A. Fujishima, H. Segawa, O. Sato, *J. Am. Chem. Soc.* **2004**, *126*, 8314 – 8319.
[11] J. Ge, Y. Hu, Y. Yin, *Angew. Chem.* **2007**, *119*, 7572 – 7575; *Angew. Chem. Int. Ed.* **2007**, *46*, 7428 – 7431.
[12] A. C. Arsenault, D. P. Puzzo, I. Manners, G. A. Ozin, *Nat. Photonics* **2007**, *1*, 468 – 472.
[13] Y. Ni, R. Rulkens, I. Manners, *J. Am. Chem. Soc.* **1996**, *126*, 4102.
[14] P. Jiang, J. F. Bertone, K. S. Hwang, V. L. Colvin, *Chem. Mater.* **1999**, *11*, 2132 – 2140.
[15] A. L. Rogach, N. A. Kotov, D. S. Koktysh, A. S. Susha, F. Caruso, *Colloids Surf. A* **2002**, *202*, 135 – 144.
[16] R. Rulkens, A. Lough, I. Manners, S. R. Lovelace, C. Grant, W. E. Geiger, *J. Am. Chem. Soc.* **1996**, *118*, 12683.
[17] K. Kulbaba, I. Manners, *Macromol. Rapid Commun.* **2001**, *22*, 711 – 724.
[18] F. Campus, P. Bonhote, M. Gratzel, S. Heinen, L. Walder, *Sol. Energy Mater. Sol. Cells* **1999**, *56*, 281 – 297.
[19] D. Cummins, G. Boschloo, M. Ryan, D. Corr, *J. Phys. Chem. B* **2000**, *104*, 11449 – 11459.

